Earthquake Engineering & Structural Dynamics
The Journal of the International Association for Earthquake Engineering

EARTHQUAKE ENGINEERING & STRUCTURAL DYNAMICS
Earthquake Engng Struct. Dyn. 2014; **43**:2075–2095
Published online 15 May 2014 in Wiley Online Library (wileyonlinelibrary.com). DOI: 10.1002/eqe.2437

Statistical models for shear strength of RC beam-column joints using machine-learning techniques

Jong-Su Jeon[1,*,†], Abdollah Shafieezadeh[2] and Reginald DesRoches[3]

[1]*School of Civil and Environmental Engineering, Georgia Institute of Technology, Atlanta, GA 30332, USA*
[2]*Department of Civil, Environmental and Geodetic Engineering, The Ohio State University, Columbus, OH 43210, USA*
[3]*School of Civil and Environmental Engineering, Georgia Institute of Technology, Atlanta, GA 30332, USA*

SUMMARY

This paper proposes a new set of probabilistic joint shear strength models using the conventional multiple linear regression method, and advanced machine-learning methods of multivariate adaptive regression splines (MARS) and symbolic regression (SR). In order to achieve high-fidelity regression models with reduced model errors and bias, this study constructs extensive experimental databases for reinforced and unreinforced concrete joints by collecting existing beam-column joint subassemblage tests from multiple sources. Various influential parameters that affect joint shear strength such as material properties, design parameters, and joint configuration are investigated through tests of statistical significance. After performing a set of regression analyses, the comparison of simulation results indicates that MARS approach is the best estimation method. Moreover, the accuracy of analytical predictions of the derived MARS model is compared with that of existing joint shear strength relationships. The comparison results show that the proposed model is more accurate compared to existing relationships. This joint shear strength prediction model can be readily implemented into joint response models for evaluation of earthquake performance and inelastic responses of building frames. Copyright © 2014 John Wiley & Sons, Ltd.

Received 9 November 2013; Revised 2 April 2014; Accepted 18 April 2014

KEY WORDS: joint shear strength; multivariate adaptive regression splines; symbolic regression; reinforced and unreinforced joint database; machine-learning methods

1. INTRODUCTION

Past earthquakes (Mexico 1985, Loma Prieta 1989, Kocaeli 1999, L'Aquila 2009) have demonstrated the importance of beam-column joint responses on the overall performance of reinforced concrete (RC) buildings. Under strong seismic loading, beam-column joints in structural systems may undergo significant deformations and loose their capacity leading to local or global damage to the structure. One of the main contributing factors to the behavior of beam-column joints is their shear strength capacity. As a result of internal moments around joints, the joint region is subjected to a joint shear demand whose magnitude is much larger than that in columns or beams. If these components are not adequately designed for shear demand, joint shear failure may occur that can be followed by lateral instability and eventually collapse of the structure [1]. This type of failure has been mainly observed in older RC buildings that lack sufficient seismic details. To investigate the sources of the potential brittle failure as well as to evaluate the seismic performance of existing RC structures, experiments have been conducted for deficient joints with pre-1967 design details [2–4]. A characteristic feature of these structures is their higher joint shear demands and higher bond stresses

*Correspondence to: Jong-Su Jeon, School of Civil and Environmental Engineering, Georgia Institute of Technology, Atlanta, GA 30332, USA.
†E-mail: jongsu.jeon@gatech.edu

compared to more recent designs. Following the poor seismic performance of pre-1967 designed structures, many experimental studies were carried out to prevent brittle joint shear failure and define acceptable earthquake performance. Results of these studies led to the establishment of joint transverse reinforcement and anchorage requirements in modern building design codes [5–7]. One of the resulting changes in the seismic design codes was the introduction of strong column–weak beam philosophy that is intended to ensure the elastic behavior of joints and the formation of plastic hinges in beams at large deformations instead of column hinging. However, significant strength and stiffness loss have been observed for joints designed based on ACI 318 Code requirements [8, 9]. Large shear forces that may be introduced by the development of the plastic hinge mechanism can cause unpredictable joint shear failure if the shear demand exceeds the joint shear strength. Therefore, reliable estimation of joint shear strength is required for both older and modern RC frame buildings. Such joint strength models must account for various influencing factors such as joint geometry, material properties, and reinforcing details.

Following the work of Hassan and Conner [10], one of the earliest experimental studies on the beam-column joint subassemblage behavior, many experimental studies have been conducted to investigate parameters that can significantly affect the joint response. Some experimental studies [8, 10, 11] stressed the importance of joint transverse reinforcement and anchorage length to retain the desirable response. Some researchers [3, 4, 12, 13] tested subassemblages without joint transverse reinforcement to evaluate the impact of shear stress on joint flexibility and damage. Leon [14] and Watanabe et al. [15] recommended limiting the diameter of beam and column longitudinal reinforcement or the ratio of member depth to rebar diameter to ensure sufficient anchorage performance. Paulay et al. [5] found that intermediate column longitudinal reinforcement significantly improved joint shear performance due to the confinement effect of the longitudinal reinforcement.

In addition to experimental studies, numerous numerical simulations have also been conducted to predict joint shear strength as well as joint response. Hwang an Lee [16, 17] proposed a softened strut-and-tie model that satisfies equilibrium, compatibility, and constitutive laws of cracked RC to estimate the shear strength of interior and exterior joints. Although the strut-and-tie model is a reliable method, it is computationally intensive because the model must satisfy the principles of mechanics of materials rigorously [18]. Park and Mosalam [19] proposed a semi-empirical equation based on the strut-and-tie method that can predict the joint shear strength of unreinforced exterior and corner beam-column joints. The proposed semi-empirical equation can reduce computational efforts by eliminating the iterative procedure, which is required in the existing strut-and-tie models to satisfy equilibrium and compatibility equations. Although their model can predict the joint shear strength for non-ductile exterior and corner joints well, their proposed formulation cannot be applied to interior or roof joints. To remedy this limitation, Park and Mosalam [20] extended the joint shear strength model of exterior or corner joints to other types of joints such as interior, roof, and knee joints. This goal was accomplished using a modification factor defined as the ratio of the joint shear strength of another joint type to that of the exterior joint defined in ASCE 41-06 provision [21]. However, because the Park and Mosalam model was validated for only four interior specimens, the model needs to be refined to reliably predict shear strength of joints with a wide range of material properties, geometric configuration, and design parameters. As another mechanistic model, the modified compression field theory (MCFT) [22] was employed by several researchers [23–25] to characterize the global response of joint panels subjected to uniform shear and uniform shear plus axial loads. However, LaFave and Shin [26] demonstrated that the MCFT may underestimate the joint shear strength for older joints. Attaalla [27] suggested an analytical formulation to evaluate joint shear strength for 61 interior and 60 exterior subassemblages exhibiting joint shear failure prior to or after beam yielding. The proposed equation reflects the most significant parameters that influence the joint behavior, and accounts for the compression-softening phenomenon associated with cracked RC. Kim and LaFave [28, 29] developed an RC joint shear strength model for a set of subassemblages with proper confinement (no out-of-plane members, and no joint eccentricity) via a Bayesian parameter estimation method, and then proposed unified joint strength model for various types of subassemblages through a stepwise removal process. The entire database consists of 212 interior, 101 exterior, and 18 knee joints, all of which exhibited joint shear failure irrespective of beam yielding, and 15 of which have joints without transverse reinforcement. Their proposed joint

DOI: 10.1002/eqe

strength model can provide reliable predictions for joints with joint transverse reinforcement; however, the model may underestimate or overestimate the shear strength for joints without transverse reinforcement, because of the limited size of deficient joints in the database.

One limitation of classical regression methods is that the functional form used in the analysis is fixed. In other words, methods such as multiple linear regression assume a simple form of relationship between the set of independent variables and dependent variable, and then determine the parameters of the model such that it best fits the data. Machine-learning methods based on pattern recognition and statistical inference can overcome this limitation by searching for the best form of the functional relationship within the optimization process in addition to model parameters. During the search process, the method can learn to improve its prediction performance based on the experiences that it gained from previous steps [30]. Machine learning has been used in a wide spectrum of applications in various fields such as social networks [31, 32], stock market analysis [33], computer vision [34], and bioinformatics [35].

From the literature review above, it is found that most of the available mechanics-based and empirical-based joint shear strength models are limited to a specific joint type (interior or exterior as well as non-ductile or ductile). Moreover, the dataset used in previous studies was limited, and the implemented probabilistic models were not able to account for complex and nonlinear relationships that may exist between independent variables and a dependent variable. These limitations may result in prediction models with relatively large uncertainties and bias for some ranges of shear strength. To reduce these uncertainties and bias in analytical predictions, this study (1) collects extensive test data of beam-column joint subassemblages for older and modern RC building frames and (2) proposes new joint shear strength models for various types of joints via the use of advanced machine-learning techniques. Many such techniques exist; among those, this study examines the application of multivariate adaptive regression splines (MARS) [36–38] and symbolic regression (SR) [39–41]. Various potential independent parameters are considered in the development of joint shear strength models. These parameters include material properties, in-plane and out-of-plane geometry, joint eccentricity, column axial load, and design parameters such as design joint stress demand and bond resistance. Finally, the comparison of the proposed joint shear strength model with that of simple multiple linear regression (MLR) as well as existing estimation methods proposed by Kim and LaFave [28, 29], Tsonos [42], and Park and Mosalam [20] demonstrates the superior performance of the proposed model.

2. MULTIPLE LINEAR REGRESSION, MULTIVARIATE ADAPTIVE REGRESSION SPLINES, AND SYMBOLIC REGRESSION MODELS

2.1. Multiple linear regression

Multiple linear regression analysis is an extension of the simple linear regression method and is used to provide a mathematical relationship between a dependent output variable (response variable) and several independent explanatory variables (predictor variables). MLR is one of the most widely used statistical methods specially for analysis of experiments where the experimenter can control predictor variables. As in simple linear regression, the basic assumption in MLR is that the error term is normally distributed with zero mean and unknown (constant) variance that is independent of the explanatory variables. Therefore, the appropriateness of an MLR model must be checked by examining the scatter-plots of the residuals against the fitted values and against the independent variable. If the scatter-plots do not exhibit any systematic pattern, the MLR model is appropriate. In addition, the normality of the distribution of the residuals must be investigated by constructing a normal probability plot. If the distribution is normal, the points in the plot will approximately follow a straight line.

Multiple linear regression is normally implemented in a stepwise fashion in which the independent variables are sequentially added to the model based on their significance until a satisfactory model is found. Thus, the main purpose of this regression method is to find significant independent variables among candidate variables that influence a dependent variable using analysis of variance (ANOVA). In ANOVA, the *F*-statistic test claims that there is no significant relationship between independent

DOI: 10.1002/eqe

variables and a dependent variable (null hypothesis), while the *t*-statistic test claims that there is no relationship between an individual independent variable and a dependent variable (null hypothesis). If a *p*-value is less than a particular significance level, the null hypothesis will be rejected. A *p*-value less than the significance level for *F*-statistic implies that at least one of the variables in the model is significant whereas for the *t*-statistic, the *p*-value less than the prescribed significance level shows that the considered independent variable is significant. Thus, stepwise linear regressions are performed until the model satisfies the condition that the *p*-value for all predictor variables in the *t*-statistic is less than the significance level. Conventionally, a reasonable significance level is 0.05 or less.

2.2. *Multivariate adaptive regression splines*

Multivariate adaptive regression splines is a form of intelligent computing regression algorithm that is proposed by Friedman [36]. This technique is a nonparametric regression methodology that is suitable for high-dimensional problems where a predictive model for a dependent variable y is to be found from a large set of independent explanatory variables, $\{x_i\}$. Unlike conventional regression techniques, MARS does not require a priori assumption regarding the functional form of the relationship between the set of predictors and the dependent output variable. This feature provides MARS with the ability to reveal complex relationships that may exist between explanatory and dependent variables; a task that is particularly challenging in high-dimensional problems. Instead, the optimal form of the functional relationship in MARS is derived within the process of regression analysis by considering a set of piecewise polynomials called splines that serve as basis functions. MARS modeling procedure partitions the space of independent explanatory variables into a set of distinct subregions and fits the aforementioned basis functions to the distinct intervals of the independent variables. Through this approach, the nonlinearity that may exist in the true underlying relationship will be approximated using separate regression models in the distinct intervals of the explanatory variables.

The output model of MARS is the summation of spline functions that can be univariate or multivariate. Univariate splines are continuous functions that are defined to be zero over a partition of the variable space and a polynomial of order m on the disjoint domain of the variable. The point within the range of the independent variable from which the spline changes from zero to a polynomial function or vice versa is called a knot. The formal definition of the splines used in MARS approach is as follows:

$$f_{bs} = [s(x-t)]_+^m \tag{1}$$

where s is a variable that takes either +1 or −1, m is the order of the polynomial that determines the degree of smoothness for the transition between the two distinct intervals. Depending on the value of s, f_{bs} is equal to

$$\begin{aligned} &if\ s=+1, then\ f_{bs} = \begin{cases} (t-x)^m & ;if\ x<t \\ 0 & ;if\ x\geq t \end{cases} \\ &if\ s=-1, then\ f_{bs} = \begin{cases} (t-x)^m & ;if\ x\geq t \\ 0 & ;if\ x<t \end{cases} \end{aligned} \tag{2}$$

Multivariate spline functions can then be generated as the products of the univariate splines. The general form of the MARS function with K basis functions, $\bar{y}_K$ is then defined as

$$\bar{y}_K(x) = \beta_0 + \sum_{k=1}^{K} \beta_k \prod_{l=0}^{L_k} \left[s_{l,k} \left(x_{v(l,k)} - t_{l,k} \right) \right]_+^m \tag{3}$$

where β_0 is a constant, β_k is the coefficients of the kth component of the regression model, L_k is the maximum number of interactions allowed for generation of basis function k, x_v is a predictor variable, and $t_{l,k}$ is the location of the knot for the lth explanatory variable of the kth regression component.

DOI: 10.1002/eqe

The model-building process of MARS is composed of two stages: a forward stepwise selection and a backward stepwise deletion process. In the forward selection process, MARS algorithm searches in a forward stepwise manner for univariate and multivariate spline basis functions that improve the model fit. The coefficients of regression, β, are found by minimizing the mean squared error (MSE) across the model space. The resulting model will be very large such that it will most likely overfit the data. To overcome this problem, the set of regression terms is pruned back in the second stage by assessing the importance of a term for the model fit. The measure of importance for the term is the amount of increase in residual squared error of the model fit upon the removal of the term from the regression model. MARS uses generalized cross-validation (GCV) criteria to find the appropriate number of terms in the final model. *GCV* is defined as

$$GCV(K) = \frac{\frac{1}{n}\sum_{i=1}^{n}[y_i - \overline{y}_K(x_i)]^2}{[1 - M(K)/n]^2} \tag{4}$$

where n is the number of observations, y_i is the target output, and $M(K)$ is the penalty function for the complexity of the model. The process of backward deletion ranks the explanatory variables based on the amount of decrease in *GCV* when the variable is removed from the regression model. The least important variable according to *GCV* criteria will be removed from the model. The backward deletion process continues until *GCV* reaches its maximum value.

2.3. Symbolic regression

Symbolic regression is a machine-learning technique proposed by Koza [39] that is capable of searching the space of analytical expressions computationally by minimizing various error metrics. Unlike conventional linear or nonlinear regression methods, SR searches for the appropriate parameters as well as the form of equations at the same time. According to the method proposed by Schmidt and Lipson [40], initial expressions are constructed by randomly combining mathematical building blocks such as arithmetic operators, trigonometric functions, constants, and state variables. Current equations are updated by recombining previous equations and by probabilistically varying their subexpressions. The algorithm holds well-fitting models, but abandons unpromising solutions. Once equations satisfy a desired level of accuracy, the algorithm terminates and returns its most parsimonious equations that most likely correspond to the intrinsic mechanisms of the observed system. Generally, SR consists of genotype or encoding. The genotype is a binary tree of algebraic operations with numerical constants and symbolic variables at its leaves. The encodings include acyclic graphs and tree-adjunct grammars. The fitness of a particular genotype (candidate model) is a numerical measure of how well it fits the experimental data in terms of its correlation or squared error of the model.

3. KEY PARAMETERS INFLUENCING JOINT SHEAR STRENGTH

This section describes the classification of joints and provides a general explanation about the mechanics of joint behavior, choice of influencing parameters, and application of existing and new statistical methods such as MLR, MARS, and SR to joint shear strength model.

3.1. Classification of beam-column joints

Beam-column joints can be classified as non-ductile and ductile joints in three different ways based on the existence of joint transverse reinforcement [28, 29], the spacing of joint transverse reinforcement [21], and the deformation ductility of subassemblages [42]. As mentioned in Section 1, Kim and LaFave [28, 29] developed a unified, simplified strength model for different types of joints, which includes three variables related to joint transverse reinforcement. For non-ductile joints (no transverse reinforcement), these variables should not be zero because the formulation was developed in a log-transformed space; thus, they used fictitious values for these variables. ASCE 41-06 [21]

DOI: 10.1002/eqe

classifies joints into older-types and modern-types and suggests a joint shear strength coefficient according to whether joint transverse reinforcement is conforming or nonconforming. Joint transverse reinforcement is conforming if hoops are spaced at half the column depth within the joint. Jeon [44] also developed non-ductile and ductile joint shear strength models following the definition of ASCE 41-06. Finally, Birely *et al.* [43] grouped older-type and modern-type joints as brittle, limited ductile, and ductile joints according to the response of subassemblages. The present study gathers existing experimental data and then develops joint shear strength models by grouping the specimens into two categories: with joint transverse reinforcement and without joint transverse reinforcement.

3.2. Significant parameters affecting beam-column joint behavior

Many experimental and analytical studies have been conducted to investigate influential parameters affecting the joint behavior such as joint strength, failure mode, and ductility. In this study, the following characteristics and design parameters are considered.

3.2.1. Concrete compressive strength. Concrete compressive strength (f_c) is one of the most important parameters for the joint shear and bond strength. The joint shear strength in the seismic codes [21, 45–47] is a function of the square root of f_c. Additionally, through statistical observations, Kim and LaFave [28, 29] showed that f_c is the most influential parameter that affects the joint shear strength.

3.2.2. Design joint shear stress. Design joint shear stress demand (τ_d) can be computed following the recommendation of ACI 352R-02 [45]:

$$\tau_d = \frac{1}{h_c b_j}\left[\alpha f_y\left(A_s^{top} + A_s^{bot}\right) - V_c\right] \tag{5}$$

where h_c is the column depth; b_j is the effective joint width, f_y is the measured yield strength of beam longitudinal reinforcement; A_s^{top} and A_s^{bot} are areas of longitudinal reinforcement in the top and bottom of beam, respectively; and V_c is the column shear force corresponding to the development of the nominal flexural strength of the beams that frame into the joint. The parameter α (stress multiplier) accounts for the hardening of the steel under earthquake loading and over strength in nominal value of f_y. For parameter α, ACI 352R-02 [45] recommends a value of 1.0 for Type 1 connections with limited deformation ductility, and 1.25 for Type 2 connections exhibiting large inelastic deformation. However, as used in Birely *et al.* [43], this study applies a unified value of $\alpha = 1.25$ to all joint types for the application of joint shear strength prediction models to real building structures with unknown failure modes (Type 1 versus Type 2). Additionally, in accordance with ACI 352R-02 [45], the parameter α can be reduced to 1.25/1.1 [43] because the actual strength of the longitudinal reinforcement is available for all specimens in the database. It is assumed that 1.1 of the 1.25 value is due to over strength, and the rest is due to strain hardening when plastic hinging occurs.

3.2.3. Bond resistance. The bond resistance of beam longitudinal reinforcement that is anchored in or is passing through the joint has a considerable impact on the response of the joint during severe seismic events. Weak bond between the longitudinal reinforcement and concrete may cause strength deterioration and excessive slippage of the reinforcement due to moment reversals. The experimental work of Hanson and Conner [10] stressed the importance of anchorage length in joints in order to maintain the ductile behavior of frames under moderate to severe earthquakes. In addition, the study by Pantelides *et al.* [4] showed that insufficient reinforcing details may result in premature anchorage failure, which significantly reduces the energy dissipation and stiffness of joints and produces large concentrated beam-end rotations. Older interior joints in which the beam longitudinal reinforcement with relatively large diameter passes through relatively small column depth are subjected to high bond stress and some bond slip during seismic actions. The bond resistance is directly related to the development length of the reinforcement, the level of joint shear stress, and the degree of confinement in the joint core. To ensure a sufficient bond resistance, ACI 352R-02 [45] recommends a minimum h_c with respect to the diameter of beam longitudinal reinforcement (ϕ_b) for interior joints with straight beam reinforcement passing through a joint panel:

DOI: 10.1002/eqe

$$\frac{h_c}{\phi_b} \geq 20\frac{f_y}{420} \geq 20 \tag{6}$$

Additionally, ACI 352R-02 [45] suggests that the development length of beam reinforcement for exterior and knee joints with beam longitudinal reinforcement terminating (with 90° hooks) within the joint region should be larger than

$$l_{dh} \geq \frac{\alpha f_y \phi_b}{6.2\sqrt{f_c}} \tag{7}$$

where l_{dh} is the actual development length in exterior joints defined per ACI 352R-02 [45]. The effect of bond resistance on the joint shear strength will be examined by considering the ratio of provided to required column depth (or anchorage length)-to-beam longitudinal reinforcement diameter (χ) so that interior and exterior joints have one consistent form. Furthermore, because of insufficient development length in exterior joints with discontinuous beam bottom reinforcement, bond failure due to rebar pullout may occur at earlier loading stages leading to significant loss of joint shear strength compared to the case of hooked rebars [4]. Thus, this study does not account for exterior joints with discontinuous beam bottom reinforcement.

3.2.4. Joint transverse reinforcement. Joint transverse reinforcement provides additional joint shear capacity to resist earthquake loading. Some experimental studies [6, 8] indicated that joint transverse reinforcement maintains a desirable ductility level of subassemblages and increases the confinement effect in the joint region. Kaku and Asakusa [11] concluded, from 18 exterior subassemblage tests, that the ductility of subassemblages improves as the amount of joint transverse reinforcement increases. ACI 352R-02 [45] recommends a minimum area and spacing of joint transverse reinforcement to ensure the ductile behavior of joints. To account for the effect of the amount of joint transverse reinforcement on joint shear strength, the metric used in this study is joint transverse reinforcement ratio (ρ_j), which is defined as the ratio of the area of the transverse reinforcement in one hoop layer in joint region (A_{sh}) to the product of the vertical spacing of the hoop (s_j) and column width (b_c).

$$\rho_j = \frac{A_{sh}}{s_j b_c} \tag{8}$$

3.2.5. In-plane and out-of-plane joint geometry. Numerous experimental results, statistical observations, and design codes reveal that in-plane geometry (*JP*) affects the joint shear strength through the confinement provided by members adjacent to the joint. Table I shows the recommended value of joint shear strength associated with in-plane geometry such as interior, exterior, and knee joints per ACI 352R-02 [45] and ASCE 41-06 [21].

The joint configuration can be changed in accordance with out-of-plane geometry, namely the existence of transverse beams (*TB*). When a joint panel initiates expansion toward the out-of-plane directions (if the joint is subjected to higher joint shear stress demand than the joint capacity), passive confinement can be activated by longitudinal reinforcement of transverse beams preventing

Table I. Code-defined values of joint shear strength associated with in-plane geometry.

	Transverse reinforcement	Interior joint	Exterior joint	Knee joint
ACI 352R-02	N.A.	$1.25\sqrt{f_c}$	$1.00\sqrt{f_c}$	$0.67\sqrt{f_c}$
ASCE 41-06	Conforming	$1.25\sqrt{f_c}$	$1.00\sqrt{f_c}$	$0.67\sqrt{f_c}$
	Nonconforming	$0.83\sqrt{f_c}$	$0.50\sqrt{f_c}$	$0.33\sqrt{f_c}$

DOI: 10.1002/eqe

the dilatation of the joint panel [28, 29]. Therefore, the out-of-plane geometry can affect joint shear strength due to this passive action. This fact can be supported by the experimental studies [2, 48] showing that the existence of transverse beams enhances the joint shear strength by as much as 20%. Kim and LaFave [28, 29] showed, from the statistical observation of an extensive test database, that (1) subassemblages with two transverse beams have a slightly higher maximum joint shear strength than those with no or one transverse beam and (2) the presence of one transverse beam has a negligible impact on the joint shear strength. Moreover, ACI 352-2R [45] and ASCE 41-06 [21] recommend the earthquake engineering community use different levels of joint shear strength for subassemblages with two transverse beams and with no or one transverse beam.

3.2.6. Member sections framing into joints. Kim and LaFave [28, 29] investigated whether the configuration of joint panel in the in-plane or out-of-plane direction influences joint shear strength. It was observed that with the increase of the ratio of beam depth to column depth (h_b/h_c), also called joint aspect ratio, and beam width to column width (b_b/b_c), the joint shear strength decreases. It should also be noted that the joint aspect ratio is one of the input variables in the models derived using the strut-and-tie approach [16, 17, 19].

3.2.7. Joint eccentricity. Joint configurations in which the beam centroid does not coincide with the column centroid are called eccentric joints. This type of joints can be generally found in the exterior frames of buildings. Raffaelle and Wight [49] showed that bending in the beam produces compression and tension forces concentrated toward the side of the joint panel associated with eccentricity. These forces may result in torsional stresses that can produce an additional shear force. Consequently, the joint eccentricity tends to reduce the joint shear strength and lateral stiffness and story shear strength and increase the severity of damage on the flush side of the joint compared to the interior side. The impact of joint eccentricity on the joint response will be examined in this study by considering the eccentricity factor (λ):

$$\lambda = 1 - \frac{e}{b_c} \tag{9}$$

where e is the distance of beam centroid to column centroid.

3.2.8. Column-to-beam flexural moment strength ratio. The moment ratio (M_R) is defined as the ratio of the summation of column nominal moment strength at a column axial (gravity) load (ΣM_{nc}) to the summation of beam nominal moment strength (ΣM_{nb}). The column moment strength is calculated per ACI 318-11 [50], and the beam moment strength is computed considering the effect of slabs only for beams with slabs. The moment ratio can be calculated as

$$M_R = \frac{\Sigma M_{nc}}{\Sigma M_{nb}} \tag{10}$$

For a desirable performance of subassemblages (strong column weak beam behavior), ACI 352-02 [45] recommends a minimum M_R of 1.2. Ehsani and Wight [6] investigated the influence of M_R on the response of exterior subassemblages under earthquake loading and concluded that the formation of plastic hinges in beams is prevented or delayed for those with M_R greater than 1.4.

3.2.9. Intermediate longitudinal reinforcement in column. Experimental observations [11, 51, 52] indicated that specimens with intermediate column longitudinal reinforcement were stronger than those without intermediate reinforcement. Hwang and Lee [16] suggested considering the contribution of column intermediate reinforcement as tension ties in the strut-and-tie mechanism. However, Park and Mosalam [20] reported that the intermediate column reinforcement does not play the role of a tension tie in the shear resisting mechanism of unreinforced exterior joints with only one central layer of intermediate column reinforcement. As in Mitra [53], the influence of the intermediate column reinforcement on the joint strength will be examined by accounting for the ratio of total intermediate column longitudinal reinforcement capacity to design joint shear demand defined previously:

DOI: 10.1002/eqe

$$\theta = 1 + \frac{A_{sc,int} f_{yc}}{\tau_d h_b b_j} \tag{11}$$

where $A_{sc,int}$ is the area of total intermediate column longitudinal reinforcement and f_{yc} is the yield strength of column longitudinal reinforcement.

3.2.10. Column axial load. There is no consensus within the research community about the effect of axial loads on the shear strength of joints. It has been argued that the axial load enhances the joint shear capacity by confining the joint core [54] and by equilibrating part of an inclined compressive strut that forms in the joint due to joint shear action [19, 55]. However, it has also been concluded that column axial load influences the joint deformation but not its shear strength [2, 7, 56]. In this study, the impact of column axial load on the joint strength will be investigated by including the column axial load factor (q):

$$q = 1 + \frac{P_c}{f_c A_g} \tag{12}$$

where P_c is the column axial load and A_g is the gross-sectional area of the column.

4. EXPERIMENTAL SUBASSEMBLAGE DATABASE

4.1. Description of database

To derive a reliable joint strength model for joints with and without joint transverse reinforcement (here referred to as reinforced and unreinforced joints, respectively), a database of laboratory testing results for 516 and 204 subassemblages with reinforced and unreinforced joints is constructed in this study. The database is created by surveying scientific literature published in the USA, Japan, New Zealand, Europe, and Korea. It includes a wide variety of materials, reinforcing details, and loading protocols. For brevity, the complete geometric and material properties of the subassemblages in the database are omitted in this paper. A detailed description of the subassemblages can be found in Jeon [44]. The experimental subassemblages include exterior and interior specimens with and without transverse beam(s) as well as specimens with and without floor slab. As plotted in Figure 1, for reinforced joints, the number of specimens with no, one, and two transverse beams is 411, 42, and 63, respectively, while for unreinforced joints, the number of specimens with no, one, and two transverse beams is 137, 32, and 35, respectively. Moreover, all of the subassemblages exhibited joint shear failure without and with yielding of members (beam or column) adjacent to the joints. Here, J, BJ, or CJ failure mode refers to joint shear failure before member yielding, joint shear failure after beam, or column yielding, respectively. For reinforced joints, the number of J, BJ, and CJ modes is 112, 85, and 7, while for unreinforced joints, the number of specimens with J, BJ, and CJ modes is 186, 318, and 1, respectively, as presented in

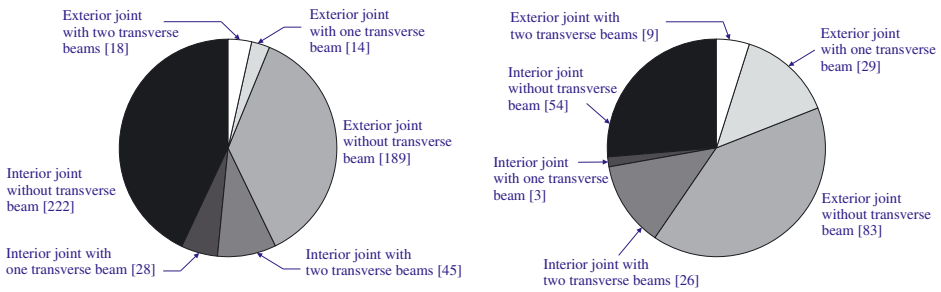

(a) Reinforced joint (b) Unreinforced joint

Figure 1. Constituents of reinforced and unreinforced joint database.

DOI: 10.1002/eqe

Table II. Moreover, for eccentric reinforced joints, the number of exterior and interior subassemblages is 1 and 41, respectively.

4.2. *Influential variables used in simulations*

The candidate input variables considered in this study are concrete compressive strength (f_c), joint transverse reinforcement ratio (ρ_j), design joint shear stress (τ_d), in-plane and out-of-plane geometry factors (*JP* and *TB*), joint panel geometry factors such as beam depth to column depth ratio (h_b/h_c) and beam width to column width ratio (b_b/b_c), joint eccentric factor (λ), column axial load factor (q), the ratio of provided to required column depth (or anchorage length) to beam rebar diameter (χ), column-to-beam nominal moment strength ratio (M_R), and the ratio of intermediate column reinforcement strength to design joint shear demand (θ). Table III presents the maximum, minimum, mean, and coefficient of variation (COV) of dependent variable (τ_{exp}) and candidate independent variables except for *JP* and *TB* for the database of reinforced and unreinforced joints. The database for unreinforced joints does not include ρ_j and λ.

5. STATISTICALLY DEVELOPED JOINT SHEAR STRENGTH MODELS

As described in the previous section, input parameters affecting joint shear strength are selected based on experimental results, statistical observations, mechanics theories, and design parameters. As employed in Kim and LaFave [28, 29] and Song *et al*. [57], this study will develop probabilistic joint shear strength models by taking the natural logarithms to (1) satisfy the homoscedasticity assumption, meaning that the dependent variable exhibits similar amounts of variance across the range of values for an independent variable and (2) reduce the nonlinearity in the relationship between the dependent and independent variables. The following section describes complete joint shear strength models derived by the three regression methods of MLR, MARS, and SR.

The basic formulation of the joint shear strength model in a log-transformed space is developed by modifying Equation (3):

Table II. Number of subassemblages with failure mode.

Database	Failure mode	Interior joint Number of transverse beams			Exterior joint Number of transverse beams		
		No	One	Two	No	One	Two
Reinforced joint	J	61	3	13	110	6	—
	BJ	160	25	32	79	8	18
	CJ	1	—	—	—	—	—
Unreinforced joint	J	24	2	9	57	20	—
	BJ	28	1	12	26	9	9
	CJ	2	—	5	—	—	—

Table III. Experimental database summary.

Database		τ_{exp} (MPa)	f_c (MPa)	ρ_j	τ_d (MPa)	h_b/h_c	b_b/b_c	λ	q	χ	M_R	θ
Reinforced joint	Min.	1.65	13.44	0.0003	2.05	0.80	0.33	0.69	1.00	0.23	0.50	1.00
	Max.	24.65	182.00	0.0238	34.70	2.00	1.00	1.00	1.81	2.19	4.13	2.86
	Mean	8.45	41.86	0.0062	10.41	1.16	0.74	0.98	1.14	0.91	1.77	1.41
	COV	0.46	0.55	0.64	0.57	0.19	0.17	0.06	0.12	0.32	0.33	0.24
Unreinforced joint	Min.	1.18	8.30	—	1.41	0.75	0.33	—	1.00	0.40	0.46	1.00
	Max.	12.15	100.80	—	28.91	2.00	1.50	—	1.59	2.33	3.80	2.48
	Mean	5.46	30.76	—	8.20	1.29	0.90	—	1.16	0.89	1.56	1.19
	COV	0.40	0.37	—	0.56	0.21	0.15	—	0.13	0.37	0.45	0.26

COV, coefficient of variation.

DOI: 10.1002/eqe

$$ln(y) = \beta_0 + \sum_{k=1}^{K} \beta_k \prod_{l=0}^{L_k} \left[s_{l,k} \left(ln\left(x_{v(l,k)} \right) - t_{l,k} \right) \right]_+^m + \varepsilon \tag{13}$$

where ε is the error term; for the reinforced database, $x_1 = f_c$, $x_2 = \rho_j$, $x_3 = \tau_d$, $x_4 = JP$, $x_5 = TB$, $x_6 = h_b/h_c$, $x_7 = b_b/b_c$, $x_8 = \lambda$, $x_9 = q$, $x_{10} = \chi$, $x_{11} = M_R$, $x_{12} = \theta$; and for the unreinforced database, $x_1 = f_c$, $x_2 = \tau_d$, $x_3 = JP$, $x_4 = TB$, $x_5 = h_b/h_c$, $x_6 = b_b/b_c$, $x_7 = q$, $x_8 = \chi$, $x_9 = M_R$, $x_{10} = \theta$.

If $L_k = 0$, $s_{l,k} = 1$, $t_{l,k} = 0$, $m = 1$, and $v = k$ in Equation (13), the formulation yields an MLR form, as expressed in Equation (14) :

$$ln(y) = \beta_0 + \sum_{i=1}^{N} \beta_i ln(x_i) + \varepsilon \tag{14}$$

where N is the number of independent variables.

5.1. Complete formulation of joint shear strength models

5.1.1. MLR. By performing a stepwise MLR based on independent variables, the final formulation for the shear strength of unreinforced joints is derived:

$$\begin{aligned} ln(\tau_{model}) = {} & 0.11 + 0.40ln(f_c) + 0.06ln\left(\rho_j\right) + 0.38ln(\tau_d) + 0.74ln(JP) + 0.92ln(TB) \\ & -0.26ln(h_b/h_c) + 0.16ln(q) + 0.09ln(\theta) \end{aligned} \tag{15}$$

The application of MLR to the unreinforced joint database yields the following relationship:

$$\begin{aligned} ln(\tau_{model}) = {} & -0.81 + 0.46ln(f_c) + 0.50ln(\tau_d) + 0.68ln(JP) + 0.62(TB) \\ & -0.25ln(h_b/h_c) + 0.08ln(M_R) + 0.14ln(\theta) \end{aligned} \tag{16}$$

where τ_{model} is the joint strength model, JP is the in-plane geometry factor ($JP = 1$ for interior joint and 0.75 for exterior joint depending on the number of members adjacent to a joint as defined in Kim and LaFave [28, 29]), and TB is the out-of-plane factor ($TB = 1.25$ for two transverse beams and 1.0 for no or one transverse beam to be consistent with ACI 352R-02 [45]). Other variables are defined in the previous section.

In the stepwise MLR procedure, an ANOVA test is carried out in a log-transformed space to develop the final joint shear strength models consisting of the significant independent variables in Equations (15) and (16). The significance level in t-statistic is generally assumed to be 0.05 for adding or removing individual independent variables. Table IV shows the p-value corresponding to each coefficient in the t-statistic, p-value in the F-statistic, and MSE. It is observed that for the reinforced and unreinforced joint database, eight and seven input variables serve as significant independent variables in the regression model, respectively. This means that all the p-values in F-statistic and in t-statistic are less than the assumed significance level. From this statistical observation, four input variables b_b/b_c, λ, χ, and M_R in the reinforced joint database and three input variables b_b/b_c, q, and χ in the unreinforced joint database are found to be insignificant independent variables. Moreover, in a log-transformed space, the coefficient of determination (R^2) for the reinforced and unreinforced joint database is 0.894 and 0.858, respectively. However, investigating the appropriateness of the MLR models is not presented because it is not the primary focus in this study.

Figure 2 depicts the comparison of the predicted and experimental joint shear strength by conducting the stepwise MLR for the reinforced and unreinforced joint database. For the reinforced joint database, the mean value (μ_Ω) and coefficient of variation (COV_Ω) of the model-to-experimental joint shear strength ratio ($\Omega = \tau_{\text{model}}/\tau_{\text{exp}}$) are 1.010 and 0.143, respectively, while for the unreinforced joint database, μ_Ω and COV_Ω are 1.012 and 0.154. These joint shear strength models provide reasonable estimate as their COV_Ω is relatively small.

DOI: 10.1002/eqe

Table IV. ANOVA results in stepwise MLR.

Reinforced joint database			Unreinforced joint database		
Input variables	*t*-statistic	*p*-value	Input variables	*t*-statistic	*p*-value
$\ln(f_c)$	24.50	0.00	$\ln(f_c)$	13.64	0.00
$\ln(\rho_j)$	5.96	0.00	$\ln(\tau_d)$	17.01	0.00
$\ln(\tau_d)$	26.52	0.00	$\ln(JP)$	6.42	0.00
$\ln(JP)$	13.93	0.00	$\ln(TB)$	4.40	0.00
$\ln(TB)$	10.59	0.00	$\ln(h_b/h_c)$	-3.67	0.00
$\ln(h_b/h_c)$	-6.18	0.00	$\ln(M_R)$	2.13	0.03
$\ln(q)$	2.74	0.01	$\ln(\theta)$	2.23	0.03
$\ln(\theta)$	2.89	0.00			
MSE = 0.0196, F = 535.53 (p-value = 0.00)			MSE = 0.0254, F = 168.99 (p-value = 0.00)		

ANOVA, analysis of variance; MLR, multiple linear regression; MSE, mean squared error.

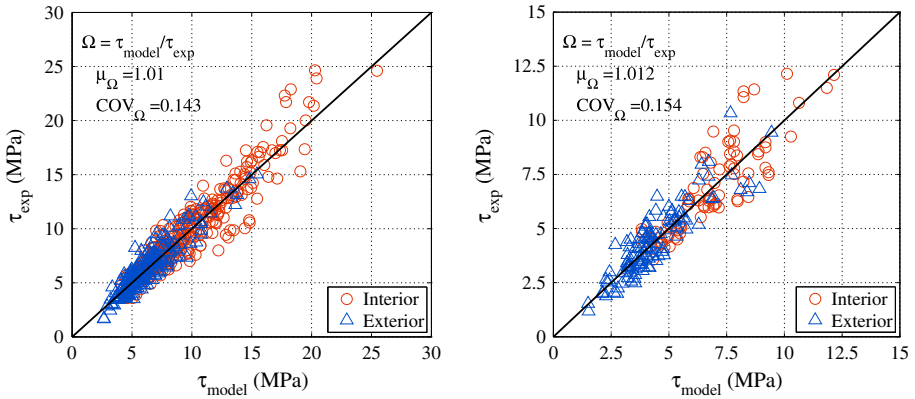

(a) Reinforced joint (b) Unreinforced joint

Figure 2. Comparison of predicted and experimental joint shear strength using multiple linear regression (MLR).

5.1.2. MARS. As previously mentioned, the final model of MARS is achieved via GCV obtained from forward selection and backward deletion process, while the final model of MLR is derived via *p*-values in the ANOVA test through either forward or backward stepwise linear regression. In addition, the MARS model not only captures complex relationships between independent and dependent variables but also does not require additional effort to verify a priori assumption about the relationship between the set of independent variables and dependent response variable. The latter feature becomes more important as the dimension of the problem increases.

All independent input variables (log-transformed) are pre-scaled into [0,1] to avoid numeric instabilities that can influence the quality of the final model associated with different locations and scales for the input variables [36]. ξ_i is the ith normalized log-transformed independent variable, which can be defined as

$$\xi_i = \frac{ln(x_i) - min(ln(x_i))}{max(ln(x_i)) - min(ln(x_i))} \tag{17}$$

Additionally, piecewise-linear and piecewise-cubic fits, widely used in the MARS method, are compared to find a more appropriate regression model in terms of accuracy and efficiency. The ANOVA decomposition is used to interpret the MARS model. This approach enables identification of particular predictor variables that enter into the model, whether they enter additively or in interactions with other predictor variables. As an illustration, the ANOVA decomposition for the MARS models for the reinforced joint database is presented in Table V. The second and third

DOI: 10.1002/eqe

Table V. ANOVA decomposition of MARS models for the reinforced joint database[§].

ANOVA function	SD		GCV		Number of basis functions	Number of parameters	Associated variables
	Linear	Cubic	Linear	Cubic			
1	0.078	0.071	0.036	0.038	2	5.0	f_c
2	0.036	0.033	0.025	0.026	2	5.0	ρ_j
3	0.171	0.159	4.816	0.081	3(2)	7.5(5.0)	τ_d
4	0.073	0.080	0.028	0.031	1	2.5	*JP*
5	0.069	0.071	0.024	0.025	1	2.5	*TB*
6	0.044	0.039	0.025	0.031	2	5.0	h_b/h_c
7	0.143	0.149	0.062	0.066	2	5.0	f_c, τ_d
8	0.106	0.127	0.031	0.041	2	5.0	ρ_j, h_b/h_c
9	0.065	0.084	0.022	0.026	1	2.5	ρ_j, b_b/b_c
10	0.039	0.035	0.020	0.020	2	5.0	τ_d, θ
11	0.055	0.043	0.022	0.021	2	5.0	*JP*, θ

ANOVA, analysis of variance; GCV, generalized cross-validation; MARS, multivariate adaptive regression splines; SD, standard deviation.
[§]Global GCV for piecewise-linear = 0.017(0.018); total number of basis function = 21(20); total effective number of parameters = 51(48.5). Note that the value in parenthesis is for piecewise-cubic.

columns in this table show the standard deviation of the function for the linear and cubic MARS models. This provides an indication of the relative importance of the function for the overall model and can be interpreted in a manner similar to a standardized regression coefficient in a linear model. The fourth and fifth columns offer another measure of importance by listing the GCV score for a model with all of the basis functions associated with the particular ANOVA function removed. This can be used to judge whether this ANOVA function makes a significant contribution to the regression model, or whether it slightly helps improve the global GCV score [36]. Judging from the second to fifth columns in the table, all ANOVA functions are survived (important to the fit) because the standard deviation and CGV for an ANOVA function are not much smaller than those for other functions. Additionally, the resulting MARS models include six individual ANOVA functions (no interaction terms) ξ_1, ξ_2, ξ_3, ξ_4, ξ_5, and ξ_6 corresponding to f_c, ρ_j, τ_d, *JP*, *TB*, and h_b/h_c, respectively, and five 2-variable interaction terms between variables ξ_1 and ξ_3, ξ_2 and ξ_6, ξ_2 and ξ_8, ξ_3 and ξ_{12}, ξ_4 and ξ_{12} which correspond to f_c and τ_d, ρ_j and h_b/h_c, ρ_j and b_b/b_c, τ_d and θ, *JP* and θ, respectively.

The global GCV of the piecewise-linear and piecewise-cubic fits is 0.017 and 0.018, respectively. Additionally, in a logarithmic space, MSE for the piecewise-linear and piecewise-cubic models is 0.0139 and 0.0149, respectively, and their respective R^2 is 0.923 and 0.918. The simulated results indicate that the piecewise-cubic model with a more complicated (flexible) form does not improve the regression fit considerably. Similarly, the linear and cubic MARS models for the unreinforced joint database are compared. It is found that the cubic MARS model does not further reduce the errors compared to the piecewise-linear model. Therefore, this study adopts the piecewise-linear MARS model for its high level of accuracy and simplicity.

On the basis of the simulated results in Table V, the complete joint shear strength model obtained from the MARS analysis is constructed for the reinforced joint database:

$$\begin{aligned} ln(\tau_{model}) = {} & 3.73 - 4.25BF_1 + 0.42BF_2 - 2.54BF_3 - 0.15BF_4 + 0.21BF_5 + 0.30BF_6 \\ & +0.61BF_7 + 0.26BF_8 + 0.97BF_9 + 1.28BF_{10} + 43.97BF_{11} + 1.28BF_{12} \\ & +0.38BF_{13} - 0.30BF_{14} - 0.44BF_{15} - 1.27BF_{16} - 5.46BF_{17} + 8.57BF_{18} \\ & +4.52BF_{19} - 5.09BF_{20} \end{aligned} \tag{18}$$

where $BF_1 = \max(0,\ \xi_3 – 0.19)$, $BF_2 = \max(0,\ \xi_1 – 0.15)$, $BF_3 = \max(0,\ 0.15 – \xi_1)$, $BF_4 = \max(0,\ 1 – \xi_4)$, $BF_5 = \max(0,\ \xi_5)$, $BF_6 = \max(0,\ \xi_6 – 0.38)$, $BF_7 = \max(0,\ 0.38 – \xi_6)$, $BF_8 = \max(0,\ \xi_2 – 0.38)$, $BF_9 = \max(0,\ 0.38 – \xi_2)$, $BF_{10} = BF_2 \cdot \max(0,\ \xi_3 – 0.18)$, $BF_{11} = BF_2 \cdot \max(0,\ 0.18 – \xi_3)$, $BF_{12} = BF_1 \cdot \max(0,\ \xi_{12} – 0.35)$, $BF_{13} = BF_1 \cdot \max(0,\ 0.35 – \xi_{12})$, $BF_{14} = BF_4 \cdot \max(0,\ \xi_{12} – 0.31)$, $BF_{15} = BF_4 \cdot \max(0,\ 0.31 – \xi_{12})$,

DOI: 10.1002/eqe

$BF_{16} = BF_6 \cdot \max(0,\ \xi_2\text{–}0.60)$, $BF_{17} = BF_6 \cdot \max(0,\ 0.60\text{–}\xi_2)$, $BF_{18} = BF_9 \cdot \max(0,\ 0.63\text{–}\xi_8)$, $BF_{19} = \max(0,\ \xi_3\text{–}0.63)$, $BF_{20} = \max(0,\ 0.63\text{–}\xi_3)$.

For the unreinforced joint database, the joint shear strength model is

$$\begin{aligned} ln(\tau_{model}) = {} & 1.73 - 4.19BF_1 - 1.43BF_2 + 1.37BF_3 - 0.71BF_4 + 0.38BF_5 + 0.26BF_6 \\ & + 4.67BF_7 + 0.57BF_8 + 0.78BF_9 - 0.25BF_{10} - 3.29BF_{11} - 1.97BF_{12} - 0.14BF_{13} \\ & - 3.45BF_{14} - 3.97BF_{14} \end{aligned} \tag{19}$$

where $BF_1 = \max(0,\ \xi_2\text{–}0.73)$, $BF_2 = \max(0,\ 0.73\text{–}\xi_2)$, $BF_3 = \max(0,\ \xi_1\text{–}0.46)$, $BF_4 = \max(0,\ 0.46\text{–}\xi_1)$, $BF_5 = \max(0,\ 0.81\text{–}\xi_5)$, $BF_6 = \max(0,\ \xi_3)$, $BF_7 = BF_6 \cdot \max(0,\ \xi_2\text{–}0.70)$, $BF_8 = \max(0,\ \xi_6\text{–}0.64)$, $BF_9 = \max(0,\ 0.64\text{–}\xi_6)$, $BF_{10} = \max(0,\ 0.48\text{–}\xi_{10})$, $BF_{11} = BF_3 \cdot \max(0,\ \xi_5\text{–}0.59)$, $BF_{12} = BF_3 \cdot \max(0,\ 0.59\text{–}\xi_5)$, $BF_{13} = BF_6 \cdot \max(0,\ 1\text{–}\xi_4)$, $BF_{14} = BF_4 \cdot \max(0,\ \xi_9\text{–}0.57)$, $BF_{15} = BF_4 \cdot \max(0,\ 0.57\text{–}\xi_9)$.

In a logarithmic space, MSE for the reinforced and unreinforced joint database is 0.0142 and 0.0155, respectively, and their respective R^2 is 0.922 and 0.910. Figure 3(a) and Figure 3(b) show the comparison of predicted and measured joint shear strength using the MARS approach for the reinforced and unreinforced joint database, respectively. For the reinforced joint database, μ_Ω and COV_Ω are 1.007 and 0.120, respectively, while for the unreinforced joint database, μ_Ω and COV_Ω are 1.008 and 0.127, respectively. Although the MARS models slightly overestimate actual experimental data, they provide highly precise results as reflected in their smaller COV_Ω.

5.1.3. SR. As mentioned in Section 2.3, SR is used to establish joint shear strength models by using the Eureqa program [40]. A small set of candidate regression models is developed with different complexity and accuracy to fit experimental data. To derive more parsimonic and accurate models, simple mathematical building blocks including algebraic operators (+, −, ×, ÷), maximum and minimum function, and constants are combined in this study. For brevity, this study selects one of candidate prediction models for reinforced and unreinforced joint database. One of the best fit reinforced joint shear strength models is given by

$$\begin{aligned} ln(\tau_{model}) = {} & 0.38 + 0.42ln(f_c) + 0.08ln\left(\rho_j\right) + 0.33ln(\tau_d) + 0.82ln(JP) + ln(TB) \\ & + ln(h_b/h_c)ln(q) + min[ln(TB)ln(\chi), ln(h_b/h_c)] - min[0.44/ln(\tau_d/\chi), ln(h_b/h_c)] \end{aligned} \tag{20}$$

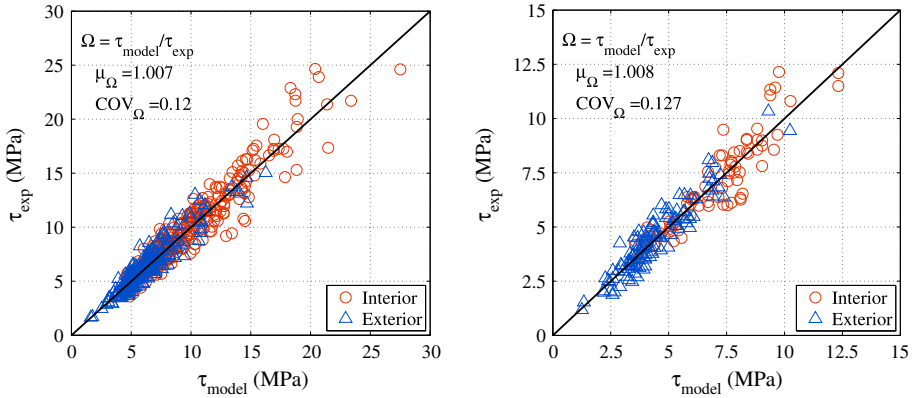

(a) Reinforced joint (b) Unreinforced joint

Figure 3. Comparison of predicted and experimental joint shear strength using multivariate adaptive regression splines (MARS).

DOI: 10.1002/eqe

In addition, one of the best candidate models for unreinforced joint database is as follows:

$$\begin{aligned} ln(\tau_{model}) = & -0.60 + 0.46ln(f_c) + 0.44ln(JP) - 1.36ln(TB) \\ & + ln(\tau_d)[0.41 + ln(TB) + 0.41min(ln(h_b/h_c), ln(\theta))] \\ & - min[0.41ln(\tau_d) - ln(JP) - ln(h_b/h_c), ln(h_b/h_c)]/ln(\tau_d) \end{aligned} \quad (21)$$

From SR in a logarithmic space, R^2 of the candidate models is 0.901 and 0.898 for the reinforced and unreinforced database, respectively, and their MSE is 0.0181 and 0.0180 for the reinforced and unreinforced joint database, respectively. Comparison of predicted and measured joint shear strength for the reinforced and unreinforced joint database is shown in Figure 4(a) and Figure 4(b), respectively. For the reinforced joint database, μ_Ω and COV_Ω are 1.024 and 0.140, respectively, whereas for the unreinforced joint database, μ_Ω and COV_Ω are 1.013 and 0.137. The simulated results indicate that the SR models predict experimental data with a high level of accuracy and precision.

5.2. *Comparison of joint shear strength models*

To choose the best estimate for predicting joint shear strength among three regression methods mentioned in Section 5.1, the simulated results are compared with regard to accuracy and precision of a model on the basis of statistical measures such as MSE, R^2, μ_Ω, and COV_Ω. Table VI summarizes the simulated results (statistical observations) obtained from three regression models for two joint databases. The table indicates that the MARS model provides the best results among them in terms of the accuracy and precision (0.0139 of MSE, 0.923 of R^2, 1.007 of μ_Ω, and 0.120 of COV_Ω for the reinforced joint database and 0.0155 of MSE, 0.910 of R^2, 1.008 of μ_Ω, and 0.127 of COV_Ω for the unreinforced joint database). The MARS model in the reinforced joint database improves the MSE, R^2, and COV_Ω in a log-transformed space, by 29% (decrease), 3% (increase), and 16% (decrease), respectively, when compared to the MLR model. Similarly, for the unreinforced joint database, MSE is decreased by 39%, R^2 increased by 6%, and COV_Ω decreased by 18% when compared to MLR. It is also observed that SR provides a more reliable prediction model than MLR; however, the SR model is not as accurate as the MARS model. This study selects the joint shear strength models obtained from MARS because they provide the highest level of accuracy and precision, although it appears to be more complicated than MLR and SR.

5.3. *Code-specified strength model based on MARS*

Code-specified shear strength models for reinforced and unreinforced joints are developed in this section. MARS approach explained in Section 5.1.2 is used to predict γ defined as the maximum

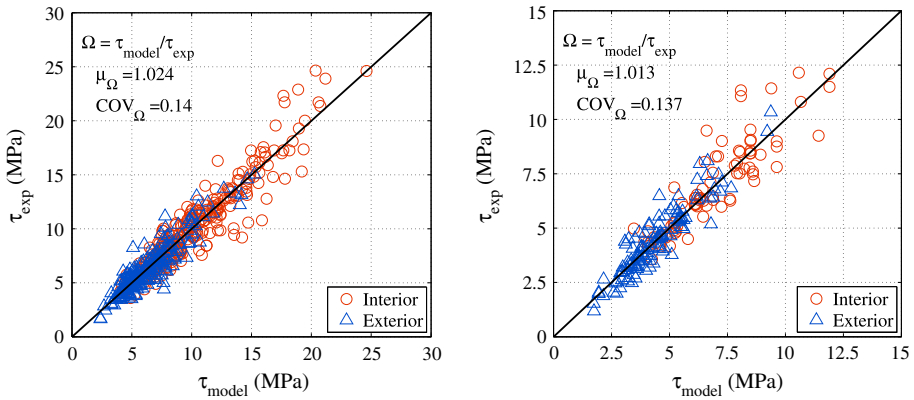

(a) Reinforced joint (b) Unreinforced joint

Figure 4. Comparison of predicted and experimental joint shear strength using symbolic regression (SR).

DOI: 10.1002/eqe

Table VI. Comparison of results for three regression methods.

Database	Method	Number of variables	Regression (logarithmic) MSE	Regression (logarithmic) R^2	τ_{model}/τ_{exp} (Ω) μ_Ω	τ_{model}/τ_{exp} (Ω) COV_Ω
Reinforced joint	MLR	8	0.0196	0.894	1.010	0.143
	MARS	8	0.0139	0.923	1.007	0.120
	SR	7	0.0181	0.901	1.024	0.140
Unreinforced joint	MLR	7	0.0254	0.858	1.012	0.154
	MARS	8	0.0155	0.910	1.008	0.127
	SR	6	0.0180	0.898	1.013	0.137

COV, coefficient of variation; MARS, multivariate adaptive regression splines; MLR, multiple linear regression; MSE, mean squared error; SR, symbolic regression.

joint shear stress divided by the square of concrete compressive strength ($\tau_{max}/\sqrt{f_c}$). For reinforced joints, the predictive formula for γ is

$$\begin{aligned} ln(\gamma_{model}) = {} & 0.46 - 0.76BF_1 - 0.27BF_2 + 0.40BF_3 - 1.04BF_4 - 0.48BF_5 + 1.06BF_6 \\ & + 0.19BF_7 + 31.97BF_8 - 3.20BF_9 + 3.46BF_{10} + 6.98BF_{11} - 0.87BF_{12} \\ & - 0.61BF_{13} + 0.68BF_{14} \end{aligned} \tag{22}$$

where $BF_1 = \max(0,\ 0.70–\xi_3)$, $BF_2 = \max(0,\ 1–\xi_2)$, $BF_3 = \max(0,\ \xi_2)$, $BF_4 = BF_1 \cdot \max(0,\ 0.93–\xi_2)$, $BF_5 = BF_1 \cdot \max(0,\ \xi_6–0.37)$, $BF_6 = BF_1 \cdot \max(0,\ 0.37–\xi_6)$, $BF_7 = \max(0,\ \xi_9–0.02)$, $BF_8 = \max(0,\ 0.02–\xi_9) \cdot \max(0,\ 0.50–\xi_6)$, $BF_9 = BF_7 \cdot \max(0,\ 0.40–\xi_{11})$, $BF_{10} = \max(0,\ \xi_3–0.70) \cdot \max(0,\ \xi_6–0.38)$ $BF_{11} = \max(0,\ \xi_3–0.70) \cdot \max(0,\ 0.38–\ \xi_6)$, $BF_{12} = BF_3 \cdot \max(0,\ \xi_6–0.60)$, $BF_{13} = BF_3 \cdot \max(0,\ 0.60–\ \xi_6)$, $BF_{14} = BF_7 \cdot \max(0,\ \xi_{12}–0.40)$.

For unreinforced joints, the value of γ is expressed as

$$\begin{aligned} ln(\gamma_{model}) = {} & 0.60 - 1.46BF_1 - 1.31BF_2 - 0.20BF_3 + 0.69BF_4 - 1.11BF_5 - 0.14BF_6 \\ & + 5.14BF_7 - 1.05BF_8 - 1.18BF_9 + 2.65 \end{aligned} \tag{23}$$

where $BF_1 = \max(0,\ 0.75–\xi_2)$, $BF_2 = \max(0,\ 0.29–\xi_5)$, $BF_3 = \max(0,\ 1–\xi_3)$, $BF_4 = \max(0,\ 0.64–\xi_6)$, $BF_5 = \max(0,\ \xi_5–0.29) \cdot \max(0,\ 0.49–\xi_{10})$, $BF_6 = \max(0,\ 1–\ \xi_4)$, $BF_7 = \max(0,\ \xi_6–0.64) \cdot \max(0,\ 0.36–\xi_8)$, $BF_8 = BF_1 \cdot \max(0,\ \xi_9–0.62)$, $BF_9 = BF_1 \cdot \max(0,\ 0.62–\ \xi_9)$, $BF_{10} = BF_1 \cdot \max(0,\ 0.40–\xi_5)$.

In a logarithmic space, MSE for the reinforced and unreinforced joint models is 0.0170 and 0.0158, respectively, and their corresponding R^2 is 0.842 and 0.888. Figure 5 depicts the comparison of code-

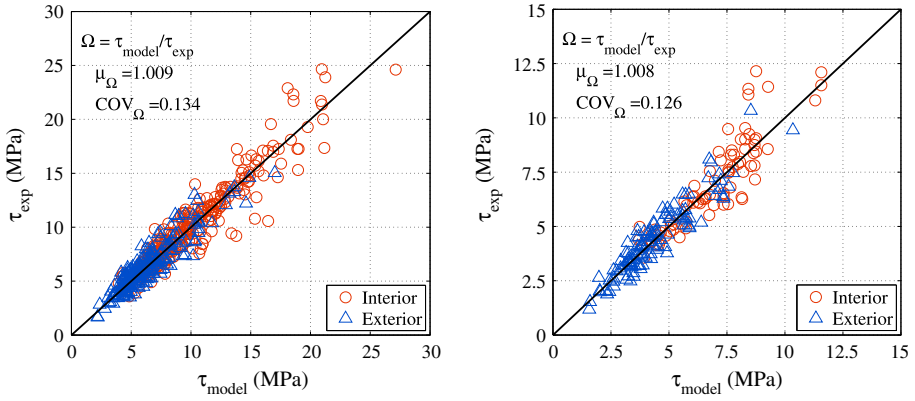

(a) Reinforced joint (b) Unreinforced joint

Figure 5. Comparison of code-specified and experimental joint shear strength using multivariate adaptive regression splines (MARS).

DOI: 10.1002/eqe

specified and measured joint shear strength for reinforced and unreinforced joints. For the reinforced joint model, μ_Ω and COV_Ω are 1.009 and 0.134, respectively, whereas for the unreinforced joint model, μ_Ω and COV_Ω are 1.008 and 0.126. Although the code-specified model for the reinforced joint database slightly increases COV_Ω compared to the model in Equation (18), the two code-specified models provide highly precise results associated with their smaller COV_Ω.

6. COMPARISON OF THE PROPOSED AND EXISTING JOINT SHEAR STRENGTH MODELS

To investigate the performance of the proposed model, this study compares the results of the proposed MARS model and existing joint shear strength models. The Bayesian and unified probabilistic models of Kim and LaFave [28, 29] (Bayesian model only for reinforced joints) and the joint strength model of Tsonos [42] are used for comparing the results for reinforced and unreinforced joints, and the semi-empirical model of Park and Mosalam [20] is employed to compare the results for the case of unreinforced joints. Figures 6 and 7 show the comparison of experimental and predicted joint shear strength by using the Kim and LaFave, Tsonos, and Park and Mosalam models, respectively. In Figure 6(a) and (b), the Kim and LaFave models for the reinforced joint database slightly overestimate joint shear strength. This comparison also indicates that the Bayesian model slightly improves the prediction with regard to μ_Ω and COV_Ω because the influential parameters were explicitly considered in this model. For the unreinforced joint database, the model overpredicts the strength for small values of joint shear strength, while it underestimates the strength for large joint shear strength values (Figure 6(c)). In Figure 7(a) and (b), for both databases, the Tsonos model for interior joints underestimates joint shear strength in the whole range of strength values, while for exterior joints the model provides acceptable predictions. Therefore, it can be concluded that the Tsonos model is an appropriate method for evaluating joint shear strength for exterior joints. Results

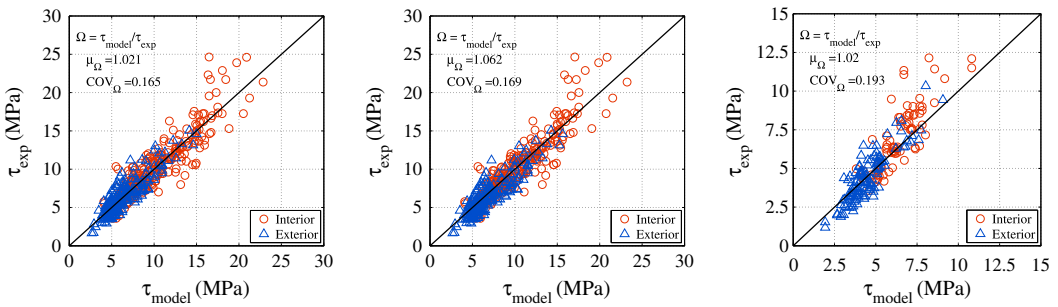

(a) Reinforced joint (Bayesian) (b) Reinforced joint (unified) (c) Unreinforced joint (unified)

Figure 6. Predicted and experimental joint shear strength using the Kim and LaFave model.

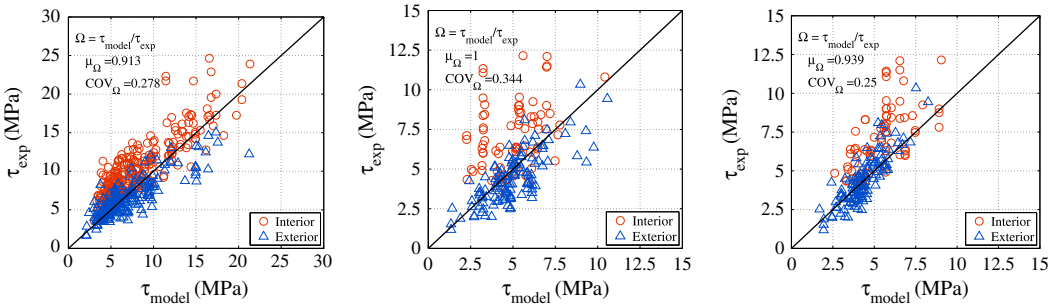

(a) Reinforced (Tsonos) (a) Unreinforced (Tsonos) (c) Unreinforced (Park and Mosalam)

Figure 7. Predicted and experimental joint shear strength using the Tsonos model and Park and Mosalam model.

DOI: 10.1002/eqe

of the Park and Mosalam model in Figure 7(c) show that the uncertainty and bias in the predictions are relatively large especially for interior joints. This is expected as their model was originally developed for exterior joints and then adopted to interior joints.

To examine the accuracy and precision of joint shear strength models, a number of quantitative measures, including root mean squared error (RMSE), correlation coefficient (ρ), μ_{Ω} and COV_{Ω} are employed. RMSE is a measure of model accuracy that represents the difference between observed and computed values in the following form:

$$\mathrm{RMSE} = \sqrt{\frac{\sum_{i=1}^{n}\left(\tau_{exp} - \tau_{model}\right)^2}{n}} \tag{24}$$

where n is the number of experimental data. A lower value of RMSE implies that the model is more accurate. ρ is a statistical measure of the degree of linear relationship between two variables (computed and measured) and is expressed as follows:

$$\rho = \sqrt{\frac{\left(\sum_{i=1}^{n}\tau_{exp}\tau_{model} - n\overline{\tau}_{exp}\overline{\tau}_{model}\right)^2}{\left(\sum_{i=1}^{n}\tau_{exp}^2 - n\overline{\tau}_{exp}^2\right)\left(\sum_{i=1}^{n}\tau_{model}^2 - n\overline{\tau}_{model}^2\right)}} \tag{25}$$

where $\overline{\tau}_{exp}$ and $\overline{\tau}_{model}$ are the mean value of experimental and computed joint shear strength, respectively. If the estimated ρ approaches to ±1, there is a strong linear relationship between the two variables. Moreover, to judge whether a predictive model overestimates or underestimates joint shear strength, Ω is calculated, and then its μ_{Ω} and COV_{Ω} are quantified to evaluate the accuracy and precision of the model, respectively.

Table VII summarizes the values of the four statistical measures for the proposed MARS model in Equations (18) and (19) as well as the Kim and LaFave, Tsonos, and Park and Mosalam models. The results indicate that the MARS model provides the highest level of accuracy and precision (lowest RMSE, lowest ρ, μ_{Ω} very close to one, and lowest COV_{Ω}) for the reinforced and unreinforced joint database compared to other existing models. In particular, the MARS model reduces COV_{Ω} by approximately 27% (Bayesian) and 29% (unified) for reinforced joints and 34% (unified) for unreinforced joints when compared to the Kim and LaFave model, the second best model with relatively accurate and precise predictions. The Kim and LaFave model provides better estimates for reinforced joints compared to unreinforced joints; the differences between the simulated results for two joint categories are relatively larger than those for the MARS model. This can be attributed to the use of a small dataset for unreinforced joints (total 15 specimens) in the Kim and LaFave model. The poorest prediction model is the Tsonos model in the sense that it has the highest RMSE, smallest ρ, and highest COV_{Ω}, particularly for unreinforced joints. This may be associated with the fact that the model validation was conducted for a relatively smaller dataset when compared to that used in this study or Kim and LaFave's research. Moreover, the Park and Mosalam model did not provide accurate and precise predictions. This can be due to the fact that their original formulation

Table VII. Comparison of error values and correlation for joint shear strength models.

Database	Model	Error, RMSE	Correlation, ρ	Mean, μ_{Ω}	COV_{Ω}
Reinforced joint	MARS	1.078	0.959	1.007	0.120
	Kim and LaFave (Bayesian)	1.425	0.927	1.021	0.165
	Kim and LaFave (unified)	1.450	0.927	1.062	0.169
	Tsonos	2.478	0.815	0.913	0.278
Unreinforced joint	MARS	0.675	0.952	1.008	0.127
	Kim and LaFave (unified)	1.065	0.899	1.020	0.193
	Tsonos	2.103	0.455	1.000	0.344
	Park and Mosalam	1.593	0.772	0.939	0.250

COV, coefficient of variation; MARS, multivariate adaptive regression splines; RMSE, root mean squared error.

DOI: 10.1002/eqe

was developed on the basis of the strut-and-tie model for exterior joints and then was modified to include other types of joints. However, their validation was limited only to a few specimens. Taking into account all of the aforementioned observations, it is seen that the simulated results demonstrate the accuracy and superiority of the proposed MARS model.

7. SUMMARY AND CONCLUSIONS

This paper proposes a set of new probabilistic joint shear strength models by employing the conventional MLR and advanced machine-learning methods of MARS and SR. Unlike the MLR, these advanced machine-learning methods can capture complex and nonlinear relationships between independent variables and a dependent variable, especially in high-dimensional problems. These features can result in smaller uncertainties and bias in prediction models. In order to enhance the reliability of the prediction models, this study collects extensive laboratory subassemblage tests with reinforced (516) and unreinforced (204) joints. Various potential independent parameters that can affect joint shear strength are considered through the review of previous experimental and analytical studies. Important observations are summarized below:

- Using a set of regression analyses, three joint shear strength models for each joint database are developed. In spite of difference in the numerical algorithms for regression analysis, significant variables used in final prediction models are found to be similar; common variables are concrete compressive strength, joint transverse reinforcement ratio (only for reinforced joins), design joint shear stress, in-plane and out-of-plane geometry factors, and joint aspect ratio.
- The simulated results from three regression models are compared with regard to accuracy and precision. For both reinforced and unreinforced joints, the MARS model among three regression methods provides the best prediction of joint shear strength because of the lowest mean squared error and highest coefficient of determination. In addition, the MARS model provides the closest mean value to unity and lowest coefficient of variation for the predicted-to-measured values (15 ~ 20% reduction in the coefficient of variation compared to the MLR model).

The performance of the proposed MARS model is further investigated by comparing the results of existing joint strength models for the entire database of the reinforced and unreinforced joints used in this study. The comparison results indicate the accuracy and superiority of the proposed MARS model in terms of error, correlation, mean value, and coefficient of variation of the predicted-to-measured joint shear strength ratio.

Because advanced machine-learning techniques that are introduced in this study have the ability to improve statistical predictions through consideration of complex dependencies of variables, they can be employed in structural engineering field to generate more reliable prediction models. Furthermore, the proposed joint shear strength model can be used to evaluate the joint capacity of existing building frames because it accounts for potential significant parameters based on material properties, design parameters, and joint configurations. Consequently, these models can be readily incorporated into joint response models for reliability assessment purposes such as seismic fragility analysis of RC building frames.

ACKNOWLEDGEMENTS

This research was supported by the National Science Foundation under NSF Grant # 1000700. However, the views expressed are solely those of the authors and may not represent the position of the NSF.

REFERENCES

1. Earthquake Engineering Research Institute (EERI). Northridge earthquake January 17, 1994, preliminary reconnaissance report. Ed. J.F. Hall. Oakland, CA, 1994.
2. Meinheit DF, Jirsa JO. Shear strength of RC beam-column connections. *ASCE Journal of the Structural Division* 1981; **107**(ST11):2227–2244.
3. Walker SG. Seismic performance of existing reinforced concrete beam-column joints. M.S. thesis, Department of Civil and Environmental Engineering, University of Washington, Seattle, WA, 2001.

DOI: 10.1002/eqe

4. Pantelides CP, Hansen J, Nadauld J, Reaveley LD. Assessment of reinforced concrete building exterior joints with substandard details. PEER Report 2002/18, Pacific Earthquake Engineering Center, University of California, Berkeley, CA, 2002.
5. Paulay T, Park R, Priestley MJN. Reinforced concrete beam-column joints under seismic actions. *ACI Journal* 1978; **75**(11):585–593.
6. Ehsani MR, Wight JK. Exterior reinforced concrete beam-to-column connections subjected to earthquake-type loading. *ACI Journal* 1985; **82**(4):492–499.
7. Fujii S, Morita S. Comparison between interior and exterior RC beam-column joint behavior. *Design of Beam-Column Joints for Seismic Resistance (SP123)*, American Concrete Institute: Detroit, MI, 1991; 145–165.
8. Durrani AJ, Wight JK. Behavior of interior beam-to-column connections under earthquake type loading. *ACI Journal* 1985; **82**(3):343–349.
9. Park R, Ruitong D. A comparison of the behavior of reinforced concrete beam-column joints designed for ductility and limited ductility. *Bulletin of the New Zealand National Society of Earthquake Engineering* 1988; **21**(4):255–278.
10. Hanson NW, Connor HW. Seismic resistance of reinforced concrete beam-column joints. *ASCE Journal of the Structural Division* 1967; **93**(ST5):533–560.
11. Kaku T, Asakusa H. Ductility estimation of exterior beam-column subassemblies in reinforced concrete frames. *Design of Beam-Column Joints for Seismic Resistance (SP123)*. American Concrete Institute: Detroit, MI, 1991; 167–185.
12. Lehman D, Stanton J, Alire D. Seismic evaluation of beam-column joints in older concrete exterior frames. *ASCE Journal of Structural Engineering* 2011; DOI: 10.1061/(ASCE)ST.1943-541X.0000463.
13. Pantelides CP, Clyde C, Reaveley LD. Performance-based evaluation of reinforced concrete building exterior joints for seismic excitation. *Earthquake Spectra* 2002; **18**(3):449–480.
14. Leon RT. Interior joints with variable anchorage lengths. *ASCE Journal of Structural Engineering* 1989; **115**(9): 2261–2275.
15. Watanabe K, Abe K, Murakawa J, Noguchi H. Strength and deformation of reinforced concrete interior beam-column joints. *Transactions of the Japan Concrete Institute* 1988; **10**:183–188.
16. Hwang S, Lee H. Analytical model for predicting shear strengths of exterior reinforced concrete beam-column joints for seismic resistance. *ACI Structural Journal* 1999; **96**(5):846–857.
17. Hwang S, Lee H. Analytical model for predicting shear strengths of interior reinforced concrete beam-column joints for seismic resistance. *ACI Structural Journal* 2000; **97**(1):35–44.
18. Hwang S-J, Lee H-J. Strength prediction for discontinuity regions by softened strut-and-tie model. *ASCE Journal of Structural Engineering* 2002; **128**(12):1519–1526.
19. Park S, Mosalam KM. Analytical model for predicting shear strength of unreinforced exterior beam-column joints. *ACI Structural Journal* 2012; **109**(2):149–160.
20. Park S, Mosalam KM. Simulation of reinforced concrete frames with nonductile beam-column joints. *Earthquake Spectra* 2013; **29**(1):233–257.
21. Elwood KJ, Matamoros AB, Wallace JW, Lehman D, Heintz JA, Mitchell AD, Moore MA, Valley MT, Lowes LN, Comartin CD, Moehle JP. Update to ASCE/SEI 41 concrete provisions. *Earthquake Spectra* 2007; **23**(3):493–523.
22. Vecchio FJ, Collins MP. The modified compression field theory for reinforced concrete elements subjected to shear. *ACI Structural Journal* 1986; **83**(2):219–231.
23. Lowes LN, Altoontash A. Modeling reinforced-concrete beam-column joints subjected to cyclic loading. *ASCE Journal of Structural Engineering* 2003; **129**(12):1686–1697.
24. Shin M, LaFave JM. Modeling of cyclic joint shear deformation contributions in RC beam-column connections to overall frame behavior, *Structural Engineering and Mechanics* 2004; **18**(5):645–669.
25. Mitra N, Lowes LN. Evaluation, calibration, verification of a reinforced concrete beam-column joint model. *ASCE Journal of Structural Engineering* 2007; **133**(1):105–120.
26. LaFave JM, Shin M. Discussion of "modeling reinforced-concrete beam-column joints subjected to cyclic loading" by Lowes LN and Altoontash A. *ASCE Journal of Structural Engineering* 2005; **131**(6):992–993.
27. Attaalla SA. General analytical model for normal shear stress of type 2 normal and high strength concrete beam-column joints. *ACI Structural Journal* 2004; **101**(1):65–75.
28. Kim J, LaFave JM. Key influence parameters for the joint shear behaviour of reinforced concrete (RC) beam–column connections. *Engineering Structures* 2007; **29**(10):2523–2539.
29. Kim J, LaFave JM. A simplified approach to joint shear behavior prediction of RC beam-column connections. *Earthquake Spectra* 2012; **28**(3):1071–1096.
30. Mjolsness E, DeCoste D. Machine learning for science: state of the art and future prospects. *Science* 2001; **293**(5537): 2051–2055.
31. Culotta A, Bekkerman R, McCallum A. Extracting social networks and contact information from email and the web, 2004.
32. Amershi S, Fogarty J, Weld D. Regroup: interactive machine learning for on-demand group creation in social networks. Proceedings of the SIGCHI Conference on Human Factors in Computing Systems, ACM, 2012; 21–30.
33. Choudhry R, Garg K. A hybrid machine learning system for stock market forecasting. *World Academy of Science, Engineering and Technology* 2008; **39**:315–318.
34. Duygulu P, Barnard K, de Freitas JF, Forsyth DA. Object recognition as machine translation: learning a lexicon for a fixed image vocabulary. In *Computer Vision-ECCV 2002*, Springer: Berlin Heidelberg, 2006; 97–112.
35. Baldi P, Brunak S. *Bioinformatics: the machine learning approach*. The MIT Press: Cambridge, MA, 2001.
36. Friedman JH. Multivariate adaptive regression splines. *The Annals of Statistics* 1991; **19**(1):1–67.

37. De Veaux RD, Psichogios DC, Ungar LH. A Comparison of two non-parametric schemes: MARS and neural networks. *Computers in Chemical Engineering* 1993; **17**:819–837.
38. Deichmann J, Eshghi A, Haughton D, Sayek S, Teebagy N. Application of multiple adaptive regression splines (MARS) in direct response modeling. *Journal of Interactive Marketing* 2002; **16**(4):15–27.
39. Koza JR. *Genetic Programming: On the Programming of Computers by Means of Natural Selection*. MIT Press: Cambridge, MA, 1992.
40. Schmidt M, Lipson H. Distilling free-form natural laws from experimental data. *Science* 2009; **324**(5923):81–85.
41. Schmidt M, Lipson H. Symbolic regression of implicit equations. *Genetic Programming Theory and Practice* 2009; **7**(5):73–85.
42. Tsonos AG. Cyclic load behavior of reinforced concrete beam-column subassemblages of modern structures. *ACI Structural Journal* 2007; **104**(4):468–478.
43. Birely AC, Lowes LN, Lehman DE. Linear analysis of concrete frames considering joint flexibility. *ACI Structural Journal* 2012; **109**(3):381–391.
44. Jeon J-S. Aftershock vulnerability assessment of damaged reinforced concrete buildings in California. Ph.D. thesis, School of Civil and Environmental Engineering, Georgia Institute of Technology, GA, 2013.
45. Joint ACI-ASCE Committee 352. *Recommendations for Design of Beam-Column Connections in Monolithic Reinforced Concrete Structures (ACI 352R-02)*. American Concrete Institute: Farmington Hills, MI, 2002.
46. Architectural Institute of Japan (AIJ). Design guideline for earthquake resistance reinforced concrete buildings based on inelastic displacement concept. Tokyo, Japan, 1999.
47. NZS 3101. Concrete structures standard. Standard Association of New Zealand, Willington, New Zealand, 1995.
48. Kitayama K, Otani S, Aoyama H. Development of design criteria for RC interior beam-column joints. *Design of Beam-Column Joints for Seismic Resistance (SP123)*, American Concrete Institute: Detroit, MI, 1991; 97–123.
49. Raffaelle GS, Wight JK. Reinforced concrete eccentric beam-column connections subjected to earthquake-type loading. *ACI Structural Journal* 1995; **92**(1):45–55.
50. ACI Committee 318. *Building Code Requirements for Structural Concrete (ACI 318-11) and Commentary*. American Concrete Institute: Farmington Hills, MI, 2011.
51. Hwang SJ, Lee HJ, Liao TF, Wang KC, Tsai HH. Role of hoops on shear strength of RC beam-column joints. *ACI Structural Journal* 2005; **102**(3):445–453.
52. Wong HF, Kuang JS. Effects of beam-column depth ratio on joint seismic behaviour. *Proceedings of the Institution of Civil Engineers - Structures and Buildings* 2008; **161**(2):91–101.
53. Mitra N. An analytical study of reinforced concrete beam-column joint behavior under seismic loading. Ph.D. thesis, Department of Civil and Environmental Engineering, University of Washington, Seattle, WA, 2007.
54. Kitayama K, Otani S, Aoyama H. Earthquake resistant design criteria for reinforced concrete interior beam-column joints. Pacific Conference on Earthquake Engineering, Wairakei, New Zealand, 1987; **1**:315–326.
55. Paulay T. Equilibrium criteria for reinforced concrete beam-column joints. *ACI Structural Journal* 1989; **86**(6):635–643.
56. Bonacci J, Pantazopoulou S. Parametric investigation of joint mechanics. *ACI Structural Journal* 1993; **90**(1):61–70.
57. Song J, Kang W-H, Kim KS, Jung S. Probabilistic shear strength models for reinforced concrete beams without shear reinforcement. *Structural Engineering and Mechanics* 2010; **34**(1):15–38.

DOI: 10.1002/eqe